DUAL SOLUTIONS OF WATER-BASED MICROPOLAR NANOFLUID FLOW OVER A SHRINKING SHEET WITH THERMAL TRANSMISSION: STABILITY ANALYSIS

***Debasish Dey*[1] and *Rupjyoti Borah*[2*]**

[1,2]Department of Mathematics, Dibrugarh University, Dibrugarh-786004, Assam, India

[2] Department of Mathematics, Tingkhong College, Dibrugarh-786612, Assam, India

Corresponding author Email: rpjtbrh@gmail.com

Investigation of the nature of dual solutions of the water-based micropolar nanofluid flow with thermal transmission due to a contracting surface has been done in the work. The flow is characterized by its shrinking velocity and imposed magnetic field. Also, this work is one of the contributions that illustrate the microrotation and microinertia descriptions of nanofluids. The effects of metallic nanoparticles Copper (Cu) *and Copper oxide* (CuO) *have been discussed throughout this study. A uniform magnetic field has been applied in the normal direction of the flow. A set of basic equations that supports the present problem are derived from the principle of conservation laws and have been modernized into a set of solvable forms by employing suitable similarity variables. The MATLAB built-in bvp4c solver scheme is engineered to solve this problem. In order to tackle boundary value problems that are highly non-linear, this numerical method largely relies on collocation and finite difference techniques. From this study, we have perceived that the speed of the motion of* $CuO - H_2O$ *nanofluid in both cases (the first and second solutions) is less than* $Cu - H_2O$ *nanofluid. The material parameter plays an important role by enhancing the heat transfer rate of the fluid at the surface of the sheet in both time-dependent and time-independent cases. From the stability analysis, the first solution has been found as the stable and physically attainable solution. Additionally, the material parameter aids in reducing the effects of couple stress and shear stress on the fluid in both situations near the surface.*

Keywords: *Nanofluid, Micropolar fluid, Heat transfer, Dual solutions, Stability analysis*

1. Introduction:

The enhancement of thermal transmission with high efficiency is a key requirement for all industries. This can be done by developing thermophysical properties like thermal conductivity and viscosity etc. The traditional techniques for developing thermal transmission are no longer valid due to some restrictions. In modern times, researchers have developed a new technique by inserting nanoparticles in some standard base fluids to enhance thermal conductivity. This technique plays an important role in different industries, as they have achieved more significant results by using nanofluids than traditional heat transfer fluids. The nanoparticles with different oxidation stages such as metallic or non-metallic particles like Cu, Al, Ag, Fe, Al_2O_3 and CuO etc that are typically used in a

base fluid like water, ethylene glycol, Kerosene and different bio-fluids. The term "Nanofluid" was first coined by Choi [1] in 1995. He observed experimentally that the nanofluid has a higher heat transfer rate than the traditional heat transfer fluids. Nanofluids are a new class of nanotechnology-based heat transfer fluids obtained by diffusing and stably deferring nanoparticles in traditional fluids. Due to the random motion of the nanoparticles suspended in base fluids, the rotation of the nanoparticles is an essential factor in the enhancement of thermal transmission. This phenomenon gives the possibility of translation and microrotation of particles. In fluid mechanics, micropolar theory exhibits this type of microrotational phenomenon. So, the applications of this fluid model containing nanoparticles can have an important significance for the enhancement of the thermal conductivity of the nanofluids. The theory of micropolar fluid flow is applied to microdevices, defectoscopy (a diagnostic method for the identification of defects) and living organisms etc.

Cu and CuO are metallic nature nanoparticles with oxidation stages 0 and 2 respectively have been focused in this study. The nanoparticles Cu and CuO can be used as catalysts, superconducting materials, sensing materials, magnetic storage media, solar energy transformation, anti-cancer formulations and detection of viruses in the human body (following Grigore *et al.* [2]) etc. Chanie *et al.* [3] have investigated the flow behaviour of water-based nanofluid containing Cu and Ag particles and found that the motion of the fluid containing Cu is more effective than the $Ag - H_2O$. Ismail *et al.* [4] have analyzed the nature of fluid flow including the nanoparticles CuO, Ag and Al_2O_3 by considering the water-based Casson fluid model. Recently, many authors, Gaikwad and Chillal [5], Prasad *et al.* [6], Muhammad *et al.* [7], Molli and Naikoti [8], Vamula *et al.* [9], Tripathi *et al.* [10] and Sadeghi *et al.* [11] have explored the importance of nanofluid flow containing Cu, Ag, Al_2O_3 and CuO etc by adopting different base fluids and geometries. Dogonchi *et al.* [12] have investigated the thermal transmission in the form of free convection and analyzed the irreversibilities of the nanofluid flow caused by a crown-wavy cavity. Tayebi *et al.* [13] have examined the entropy generation of the nanofluid that flows in an annular region. Seyyedi *et al.* [14] have analyzed the second law of thermodynamics under the influence of nanoparticles in a magnetized convective fluid. Krishna and Chamkha [15] have studied the hall effects on the magnetized water-based nanofluid flow between two parallel disks and their practical applications.

The theory of micropolar fluid was first introduced by Eringen [16]. He gave different physical significance of this fluid model. Ariman *et al.* [17] and Anuradha and Punithavalli [18] have studied fluid flow problems using the micropolar fluid model with different geometries. Krishna *et al.* [19] have investigated the simultaneous effects of both thermal and mass transmissions of the micropolar fluid flow caused by an absorbent surface under the influence of a magnetic field and hall effects. Hussain *et al.* [20], Liana *et al.* [21], Maripala and Naikoti [22], Alizadeh *et al.* [23], Dawar *et al.* [24] and Saleem *et al.* [25] etc have studied micropolar model-based fluid flow containing nanoparticles by adopting different geometries. However, they have looked into the issues with

micropolar nanofluid flow in the presence of various nanoparticles, but they haven't looked into the duel solutions and their stability when taking into account nanoparticles Cu and CuO.

The magnetized fluid flow problems associated with thermal and mass transmissions caused by extending or contracting geometries have taken a great deal of interest in modern research areas such as medical sciences, engineering sciences, geophysics and many other fields. Annealing and thickening of copper wire are the most important industrial applications of this type of geometry for heat and mass transfers. Although this type of geometry with the influence of a magnetic field occurs frequently in manufacturing involving hot metal rolling, wire drawing, glass fiber production, metal spinning and magnetic separation etc. Recently, Tayebi *et al.* [26], Chamkha *et al.* [27] and Krishna and Chamkha [28, 29] have investigated the magneto-hydrodynamic effects on the different fluid models by considering different geometries. Crane [30] was the first author to explore the idea of fluid flow problems on account of this geometry. In the last five years, many researchers, including Khan *et al.* [31], Vamula *et al.* [9], Ghosh and Mukhopadhyay [32], Dey and Borah [33], Dey *et al.* [34], Dey and Chutia [35], Zehra *et al.* [36], Prasannakumara [37] and Jamshed *et al.* [38] have investigated the fluid flow problems caused by the present geometry by considering different fluid models. By taking nanofluid into account because of its stretching surface, the aforementioned authors have explored many fluid models, including Casson fluid, Maxwell fluid, and Newtonian fluid, among others. However, due to a diminishing surface, they have not examined the nature of dual solutions by taking the micropolar nanofluid model into account.

Due to the irregular behaviour of surfaces in the considering geometries and the lack of mathematical tools and assumptions, some initial complexity in the flow is observed, which develops non-unique flow solutions. This initial disturbance in the flow characterizes the flow solutions into two categories; one of them converses into the steady flow solution much faster than the others. Stability analysis of the dual solutions is mandatory for characterizing the stable and physically tractable solution. Markin [39] was the first author to investigate the existence of double solutions and their characteristics. Anuar and Bachok [40] have investigated the existence of dual solutions of nanofluids by considering the present fluid model. Recently, Ghosh and Mukhopadhyay [32], Dey and Borah [41], Dey *et al.* [42], Waini *et al.* [43] and Khashi'e *et al.* [44] have explored the nature of non-uniqueness solutions and their stability behaviour by considering different fluid model. The aforementioned researchers have not studied the characteristics of dual solutions by considering the micropolar nanofluid model with the inserted naoparticles Cu and CuO.

The prime objective of the present problem is to study the non-uniqueness of flow solutions and their stability in the water-based micropolar nanofluid flow caused by a contracting surface with thermal transmission. The metallic nanoparticles Cu and CuO are considered here under the influence of MHD. A homogeneous magnetic field is applied in the normal direction of the flow. The basic equations that support the present problem are modernized into solvable form by employing a set of

suitable similarity variables. Due to the non-linear behaviour of the problem, a numerical method called the "MATLAB built-in bvp4c solver scheme" is adopted to solve this problem. It is a finite difference code that implements three-stage Lobatto IIIa formula. A representative set of numerical results is analyzed graphically and the numerical values of the physical quantities are presented in tabular form. A stability analysis is executed to distinguish the stable and physically attainable solutions. A comparison has been done with the previously published paper reported in Liana *et al.* [21] to determine the conformity of the present codes. The major findings of this study are that the material parameter that is responsible for micropolar fluid regulates the influence of shear stress and couple stress on the fluid in the vicinity of the surface. Also, there are two types of solutions that arise; one of them is stable and physically achievable. This fluid model and the considering geometry have multifarious applications in different physical fields. From the stability analysis, the first solution is stable and physically attainable solution. This type of fluid model is generally important for industrial applications because the mixing of nanoparticles in a convective fluid enriches the heat transfer rate. The present nanoparticles, under the influence of a magnetic field, have been applied as dietary additives, lubricant supplements, chemical sensors, biomedical, pharmaceutical and cosmetic energy etc.

We were able to ascertain via the literature review that this study is novel and will have a significant influence on other experts in the field. To the best of the authors' knowledge, micropolar fluid has not yet been taken into account while analyzing dual solutions and their stability on the MHD boundary-layer flow of water-based nanofluid due to a shrinking surface in the presence of heat transmission. While, Liana *et al.* [21] have investigated the micropolar nanofluid flow due to a stretching surface by inserting different nanoparticles. But we have analyzed the dual solutions and their stability by considering Liana *et al.'s* [21] fluid model using a shrinking surface and different nanoparticles such as Cu and CuO with the help of a numerical technique called the MATLAB built-in bvp4c.

2. Mathematical Formulation:

The two-dimensional, incompressible and time-independent MHD boundary layer flow of water-based micropolar nanofluid caused due to a shrinking sheet is considered. The fluid flow is characterized by the stretching velocity $u_w(x) = cx$, where the constant $c > 0$ signifies stretch of the sheet and $c < 0$ represents the shrinking surface with prescribed wall temperature T_w and microrotation component (N) normal to the $xy-$ plane. u and v are the velocity components along the parallel$(x-\text{direction})$ and normal $(y-\text{direction})$ directions of the flow. A constant magnetic field B_0 is employed into the perpendicular direction of the flow. The flow is imprisoned to $y > 0$ and the boundary layer separation will be formed due to the horizontal motion of the fluid. The wall is characterized by the mass transfer velocity $v_w = v_0$ such that $v_0 > 0$ signifies suction and $v_0 < 0$

represents an injection of the flow. Here, the metallic quality nanoparticles Cu and Cu are considered. The schematic diagram which represents this problem is shown in Fig. 1.

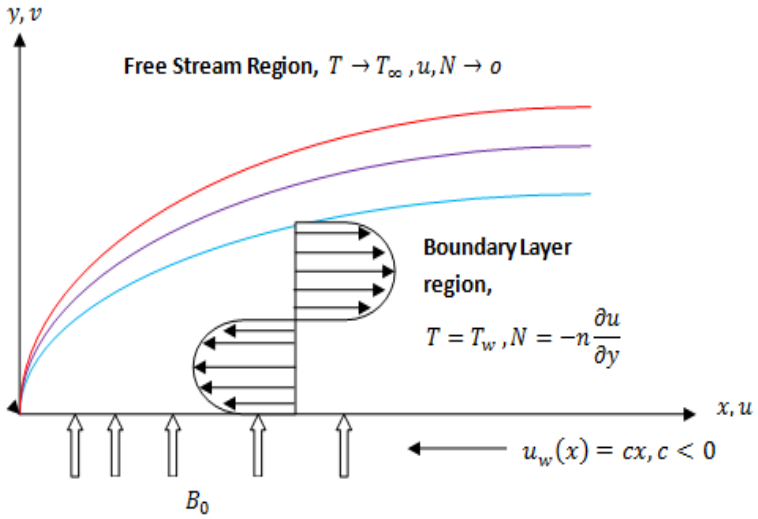

Figure 1. Schematic diagram of the problem.

Applying the aforementioned boundary-layer assumptions together with the principle of conservation of mass, linear momentum, angular momentum and energy, the following set of governing equations has been derived. The other assumptions are given below:

1. The flow is governed by the inertia force, viscous force, microrotational force and Lorentz force.
2. The angular momentum equation is maintained by the conservation of angular momentum.
3. In heat transfer, the flow is maintained by the free convection, conduction and Joule heating.

Also, using the nanofluid model anticipated by Liana *et al.* [21] and Hussain *et al.* [20], the mathematical representation of this present problem is given below:

$$\frac{\partial u}{\partial x}+\frac{\partial v}{\partial y}=0, \tag{1}$$

$$u\frac{\partial u}{\partial x}+v\frac{\partial u}{\partial y}=\left(\frac{\mu_{nf}+k}{\rho_{nf}}\right)\frac{\partial^2 u}{\partial y^2}+\frac{k}{\rho_{nf}}\frac{\partial N}{\partial y}-\frac{\sigma_{nf}B_0^2}{\rho_{nf}}u, \tag{2}$$

$$\rho_{nf}j\left(u\frac{\partial N}{\partial x}+v\frac{\partial N}{\partial y}\right)=\gamma_{nf}\frac{\partial^2 N}{\partial y^2}-k\left(2N+\frac{\partial u}{\partial y}\right), \tag{3}$$

$$u\frac{\partial T}{\partial x}+v\frac{\partial T}{\partial y}=\alpha_{nf}\frac{\partial^2 T}{\partial y^2}+\frac{\sigma_{nf}B_0^2}{(\rho C_P)_{nf}}u^2. \tag{4}$$

The related boundary restrictions are:

$$y=0: v=v_0, u=u_w(x)=cx, N=-n\frac{\partial u}{\partial y}, T=T_w;$$

$$y\to\infty: u\to 0, N\to 0, T\to T_\infty. \tag{5}$$

Where, $0\le n\le 1$ is the constant such that $n=0$ signifies $N=0$ at the wall, physically signifies the concentrated particle flows in which the density of the particle is significantly large that of

microelements near the wall are unable to rotate and $n = 1$ gives turbulent boundary layer (Ahmadi and Shahinpoor [45]). In this study, we have considered $n = 0.5$ which physically corresponds to vanish the anti symmetric part of the stress tensor and gives the weak concentration of microelements.$K = \frac{k}{\mu_f}$ is responsible for micropolar fluid termed as material parameter.

The thermophysical properties and their standard values are presented in Table-1. The parameters $\mu_{nf}, \rho_{nf}, \sigma_{nf}, \gamma_{nf,} \alpha_{nf}, K_{nf}$ and $(\rho C_p)_{nf}$ can be defined in the following standard forms (referring Liana *et al.* [21], Hussain *et al.* [20], Ahmed *et al.* [46] and Togun *et al.* [48]):

$$\mu_{nf} = \mu_f(1-\phi)^{-2.5}, \rho_{nf} = (1-\phi)\rho_f + \phi\rho_s, \sigma_{nf} = \sigma_f\left(1 + \frac{(3(\sigma-1)\phi)}{2+\sigma-(\sigma-1)\phi}\right),$$

$$\gamma_{nf} = \left(\mu_{nf} + \frac{K}{2}\right)j, \alpha_{nf} = \frac{k_{nf}}{(\rho C_p)_{nf}}, k_{nf} = k_f\left(\frac{k_s+2k_f-2\phi(k_f-k_s)}{k_s+2k_f+\phi(k_f-k_s)}\right),$$

$$(\rho C_p)_{nf} = (1-\phi)(\rho C_p)_f + \phi(\rho C_p)_s. \tag{6}$$

To solve the above governing equations, the following set of similarity transformation which satisfies the equation (1) is used. This transformation renovates the governing equations into a solvable form.

$$\Psi = \sqrt{\nu_f c}\, xf(\eta), N = c\sqrt{c\nu_f}\, xg(\eta), \eta = y\sqrt{\frac{c}{\nu_f}}, \theta(\eta) = \frac{T-T_\infty}{T_w-T_\infty}, s = -\frac{v_0}{\sqrt{c\nu_f}}, Pr = \frac{\nu_f}{\alpha_f},$$

$$M = \frac{\sigma_f B_0^2}{\rho_f c}, K = \frac{k}{\mu_f}, Ec = \frac{u_w^2}{C_p(T_w-T_\infty)}. \tag{7}$$

Employing equation (7) into the equations (2)-(4), we have achieved the following normal form:

$$Af'''(\eta) + f(\eta)f''(\eta) - f'(\eta)^2 - BMf'(\eta) + Cg'(\eta) = 0, \tag{8}$$

$$Dg''(\eta) + f(\eta)g'(\eta) - f'(\eta)g(\eta) - C[2g(\eta) + f''(\eta)] = 0, \tag{9}$$

$$E\theta''(\eta) + Prf(\eta)\theta'(\eta) + PrEcMf'^2 = 0. \tag{10}$$

Where, the superscript " $'$ " represents the differentiation with respect to η.

The boundary conditions (5) becomes:

$$f(0) = s, f'(0) = \lambda, g(0) = -nf''(0), \theta(0) = 1;$$

$$f'(\infty) \to 0, g(\infty) \to 0, \theta(\infty) \to 0. \tag{11}$$

Where, the constant $A, B, C, D\&E$ are defined in the following way:

$$A = \frac{\left(\frac{\mu_{nf}}{\mu_f}+K\right)}{\left((1-\phi)+\phi\left(\frac{\rho_s}{\rho_f}\right)\right)}, B = \frac{\rho_f\sigma_{nf}}{\rho_{nf}\sigma_f}, C = \frac{K}{(1-\phi)+\phi\left(\frac{\rho_s}{\rho_f}\right)}, D = \frac{\left(\frac{\mu_{nf}}{\mu_f}+\frac{K}{2}\right)}{\left((1-\phi)+\phi\left(\frac{\rho_s}{\rho_f}\right)\right)}, \; E = \frac{\left(\frac{k_{nf}}{k_f}\right)}{(1-\phi)+\phi\left[\frac{(\rho Cp)_s}{(\rho Cp)_f}\right]}\&$$

$$s = -v_0(c\nu_f)^{-0.5}.$$

Some important physical quantities of interest are observed in this study. These quantities are drag force (C_f), couple stress (C_n) and heat transfer rate (Nu) at the surface and are defined in the following way:

$$C_f = \frac{\left[(\mu_{nf}+K)\left[\frac{\partial u}{\partial y}\right]_{y=0} + k(N)_{y=0}\right]}{\rho_{nf}u_w^2}, C_n = \frac{x}{a}\left(\frac{\partial N}{\partial y}\right)_{y=0}, Nu = -x\left(\frac{\partial T}{\partial y}\right)_{y=0}(T_w - T_\infty)^{-1}. \quad (12)$$

Using equation (7), we have got the following dimensionless physical quantities:

$$C_f = Re_x^{-\frac{1}{2}}[1 + (1-n)K]f''(0), C_n = Re_x g'(0), Nu = -Re_x^{\frac{1}{2}}\theta'(0). \quad (13)$$

Where, $Re_x = \frac{u_w x}{\nu_f}$ is the local Reynolds number.

2.1 Stability Analysis:

In the initial position of the surface, there are no any disturbances in the flow. But, when the surface is contracted along the flow direction then some initial disturbances have been observed which are dependent on time. During this situation, the flow solutions have been categorized into two parts, one of them is stable and another one is unstable according to the flow disturbances grow or decay with time. A stability analysis is important to characterize the stable or unstable flow solutions between the two solutions. To implement the stability analysis on this problem, time-dependent governing equations are needed. So, we have achieved the time-dependent governing equations by adding the terms $\frac{\partial u}{\partial t}, \frac{\partial N}{\partial t}$ and $\frac{\partial T}{\partial t}$ into the equations (2), (3) and (4) respectively. Due to the presence of time variable, equation (7) takes a modified form as given below:

$$\Psi = \sqrt{\nu_f c}\, x f(\eta,\tau), N = c\sqrt{c\nu_f}\, x g(\eta,\tau), \eta = y\sqrt{\frac{c}{\nu_f}}, \theta(\eta,\tau) = \frac{T-T_\infty}{T_w-T_\infty}, \tau = ct. \quad (14)$$

The time-dependent governing equations after using equation (14) become:

$$A\frac{\partial^3 f}{\partial \eta^3} + f\frac{\partial^2 f}{\partial \eta^2} - \left(\frac{\partial f}{\partial \eta}\right)^2 - BM\frac{\partial f}{\partial \eta} + C\frac{\partial g}{\partial \eta} - \frac{\partial^2 f}{\partial \eta \partial \tau} = 0, \quad (15)$$

$$D\frac{\partial^2 g}{\partial \eta^2} + f\frac{\partial g}{\partial \eta} - \frac{\partial f}{\partial \eta}g - C\left[2g + \frac{\partial^2 f}{\partial \eta^2}\right] - \frac{\partial g}{\partial \tau} = 0, \quad (16)$$

$$E\frac{\partial^2 \theta}{\partial \eta^2} + Prf\frac{\partial \theta}{\partial \eta} + PrEcM\left(\frac{\partial f}{\partial \eta}\right)^2 - \mathrm{Pr}\frac{\partial \theta}{\partial \tau} = 0. \quad (17)$$

Related boundary restrictions are:

$$f(0,\tau) = s, \frac{\partial f(0,\tau)}{\partial \eta} = \lambda, g(0,\tau) = -n\frac{\partial^2 f(0,\tau)}{\partial \eta^2}, \theta(0,\tau) = 1;$$

$$\frac{\partial f(\infty,\tau)}{\partial \eta} \to 0, g(\infty,\tau) \to 0, \theta(\infty,\tau) \to 0. \quad (18)$$

To test the stability of the steady flow solution, $f(\eta) = f_0, g(\eta) = g_0$ and $\theta(\eta) = \theta_0$ fulfilling the equations (8)-(10), a set of perturb equations is considered for separating the variables (following Markin [39], Dey and Borah ([33], [41]) and Dey *et al.* [42]):

$$f(\eta,\tau) = f_0(\eta) + e^{-\omega\tau}F(\eta),$$

$$g(\eta,\tau) = g_0(\eta) + e^{-\omega\tau}G(\eta), \tag{19}$$

$$\theta(\eta,\tau) = \theta_0(\eta) + e^{-\omega\tau}H(\eta).$$

Where, ω is an unknown eigenvalue parameter, F, G and H the small related to f_0, g_0 and θ_0. Inserting equation (19) into equations (15)-(17), fixing $\tau \to 0$ and simplifying the equations, we have achieved the following linearized eigenvalue problems.

$$AF''' + f_0F'' + f_0''F - 2f_0'F' - BMF' + CG' + \omega F' = 0, \tag{20}$$

$$DG'' + (f_0G' + g_0'F) - (g_0F' + f_0'G) - C(2G + F'') + \omega G = 0, \tag{21}$$

$$EH'' + \Pr(f_0H' + \theta_0'F) + 2PrEcMf_0'F' + Pr\omega H = 0, \tag{22}$$

relevant boundary restrictions are:

$$F(0) = 0, F'(0) = 0, G(0) = 0, H(0) = 0; \tag{23}$$

$$F'(\infty) \to 0, G(\infty) \to 0, H(\infty) \to 0.$$

Following Mishra *et al.* [47] and Dey and Borah [33], the equations (20)-(22) are solved together with adjusted boundary conditions (referring Dey *et al.* [49]). It is noticed that this eigenvalue problem gives an infinite number of eigenvalues $\omega_1 < \omega_2 < \omega_3 < \cdots$, where ω_1 signifies a least eigenvalue. The stability of the solution can be analyzed with the help of the smallest eigenvalue. If $\omega_1 > 0$, then the initial complexity in the flow decline with time and converges to its steady flow solution and hence the flow solution is stable and physically attainable. Otherwise, the flow solution to be unstable due to the escalation of complexity in the flow with time.

Table-1. Thermo-physical properties of water-based nanoparticles (referring Hussain *et al.*[14], Chanie *et al.*[3], Ismail *et al.*[4] and Togun *et al.* [48]).

Physical Properties	**Water (H_2O)**	**Cu**	**CuO**
$\rho(Kgm^{-3})$	997.1	8933	6320
$C_p(J(Kg.K)^{-1})$	4179	385	531.6
$K(W(M.K)^{-1})$	0.6130	401	76.5
$\sigma(sm^{-1})$	5.5×10^{-6}	59.6×10^{6}	6.9×10^{-2}

2.2 Methodology:

In accordance with Dey and Chetia [35], the MATLAB built-in bvp4c solver scheme is used to numerically solve the non-linear coupled equations (8–10) and (20–22), along with the boundary limitations (11) and (23). It uses a finite difference algorithm to carry out the three-stage Lobatto IIIa formula and impose the collocation method for finding solutions to the problem. To solve boundary value problems using this scheme, the users have to execute three functions: a set of initial guess solutions, a set of first-order differential equations and a set of boundary restrictions. By introducing a set of new variables, the users may convert the higher-order differential equations into first-order differential equations, as described in Dey *et al.* [34]. The existing methods and the present method are both numerical methods to solve boundary value problems. But there are some factors that can make bvp4c superior to the existing methods. These factors are:

1. BVP4C can handle problems with multiple solutions more naturally than the shooting method.
2. BVP4C gives higher-order accuracy results than others.
3. BVP4C can be easier to use for new users.

3. Results and Discussion:

To investigate the flow nature with different flow parameters of this problem, the MATLAB built-in bvp4c solver scheme is employed. This investigation has been done to study the nature of dual solution with the influence of different flow parameters such as M, K and ϕ of the micropolar model-based nanofluid. A representative set of numerical results are demonstrated pictorially in Figs. (2)-(10) and in tabular form. In this discussion, the values of the flow parameters are taken as $M = 0.5, Pr = 7, K = 0.5, s = 1.23, \lambda = -0.5, Ec = 10$ and $\phi = 0.05$, unless otherwise stated. In the figures, two types of solutions are observed, the solid line represents the first solution which is responsible for converging significantly faster solutions asymptotically and the dashed line signifies the second solution which is converged slowly asymptotically. Before conferring the numerical results, we afford confirmation of our numerical code by solving the model presented in Liana *et al.* [21] and comparing the present numerical results (first solution) with the results reported in Liana *et al.* [21]. Table-2 is a comparison result and found a good conformity of our results.

Table-2. Values of skin friction coefficient $-f''(0)$ for various values of s and ϕ when $K = 2, n = 0.5, M = 0, Pr = 0, Ec = 0$ and $\lambda = 1$ (stretching sheet).

s	ϕ	**Skin friction coefficient $(-f''(0))$ for $Cu - H_2O$**	
		Liana *et al.*[21] (shooting method solution)	Present results (bvp4c solver solution)
0	0.05	-1. 6258	-1.6220
1		-2.4026	-2.4120
2		-3.3896	-3.3006
0	0.1	-1.7726	-1.7712
	0.2	-1.9466	-1.9261

The figures (2)-(4) are depicted to show the influence of M on the velocity, angular velocity and temperature distributions of the electrically conducting nanofluid. From Fig. 2, it is discerned that the magnitude of the fluid velocity during both the solutions decelerates with developing values of M. It can be physically described that enhancing values of M produces a resistance force called Lorentz force that oppose the motion of the fluid. This means that the fluid experiences resistance to its motion by the influence of Lorentz force. Also, it is noticed that the magnitude of the fluid containing the nanoparticle CuO (Copper with oxidation stage 2) has larger velocity than the fluid containing the nanoparticle Cu (Copper with oxidation stage 0). This Cu nanoparticle actually slows down the fluid in comparison to CuO. But, it reduces the angular velocity distribution during both the solutions of the fluid [see Fig. 3]. It is also observed that the angular velocity distributions of the first and second solutions of the $CuO - H_2O$ is larger than $Cu - H_2O$. When the Lorentz force acts on the fluid elements, it generates a torque on them. This torque opposes the rotation of the fluid. As a result of the torque generated by the Lorentz force, the angular momentum of the fluid is affected and hence the angular velocity of the fluid has been reduced. Due to the effects of M, the thermal transmission of

the nanofluid is enhanced in both the cases. Again, the fluid containing nanoparticle Cu has high thermal transmission capacity than the fluid containing the nanoparticle CuO [See Fig. 4]. It can be physically explained that application of magnetic parameter develops the frictional force of the fluid, as a result additional heat is generated. This means that the thermal transmission of the fluid develops due to the influence of the magnetic parameter.

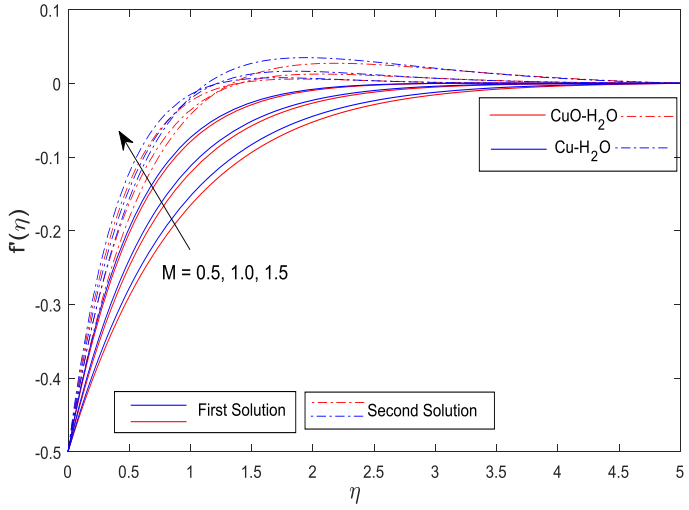

Figure 2. Velocity distribution $f'(\eta)$ for developing values of M.

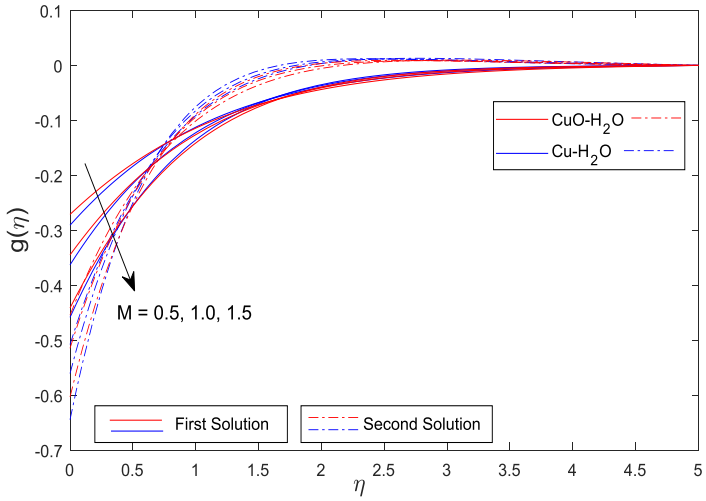

Figure 3. Angular velocity distribution $g(\eta)$ for developing values of M.

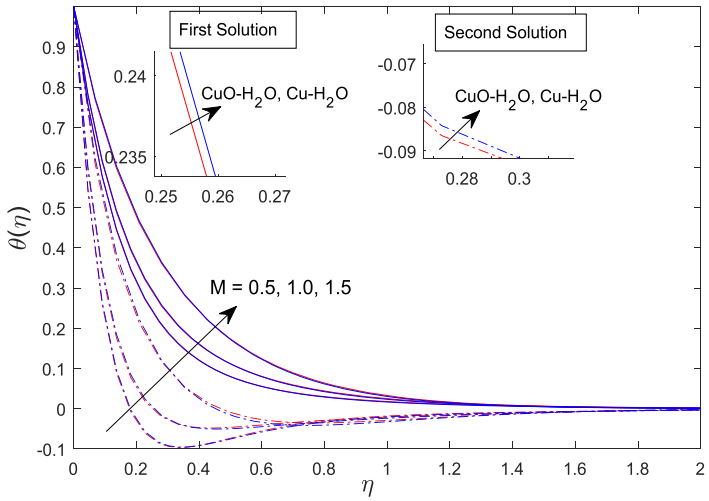

Figure 4. Temperature distribution $\theta(\eta)$ for developing values of M.

The figures (5)-(7) are presented for the influence of material parameter (K) which is responsible for the micropolar fluid model on the velocity, angular velocity and temperature distributions of the nanofluid containing the nanoparticles Cu and CuO. It is seen from Fig. 5 that we can control the motion of the nanofluid by improving the values of K. It is also perceived that the magnitude of the velocity distribution of $CuO - H_2O$ in both the cases (first and second solutions) is superior to $Cu - H_2O$. It can be physically explained that an increase in the material parameter (K) in the micropolar fluid accelerate the fluid motion. The improving values of K reduces the magnitude of the angular velocity of the nanofluid and maximum variation is observed near the surface of the sheet. Also, a higher magnitude of the angular velocity distribution is observed of the fluid containing Cu in both the solutions [see Fig. 6]. The reason behind this phenomenon is that the increasing values of K result in a larger microrotation viscosity, which suggests that the fluid encounters more internal friction or resistance to internal motion. Because of the internal friction, small-scale vortices in the fluid are less likely to form and spread, which ultimately results in a decrease in the fluid's total rotational velocity. Again, this parameter reduces the temperature distribution in both the cases of the nanofluid which is seen in Fig. 7. The temperature distribution of the fluid containing nanoparticle CuO is smaller than Cu. That is the nanofluid containing pure nanoparticle Cu has higher thermal transmission during both first and second solutions.

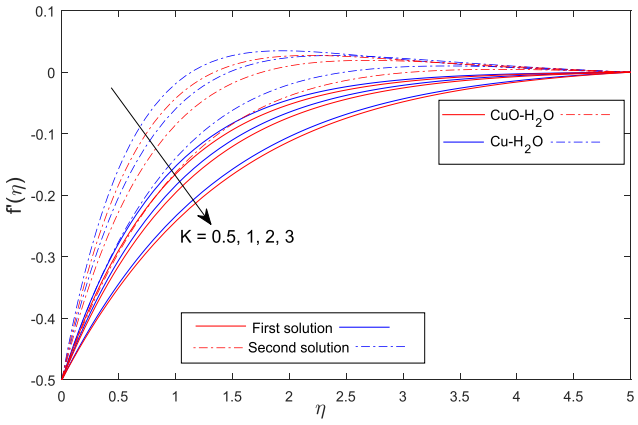

Figure 5. Velocity distribution $f'(\eta)$ for developing values of K.

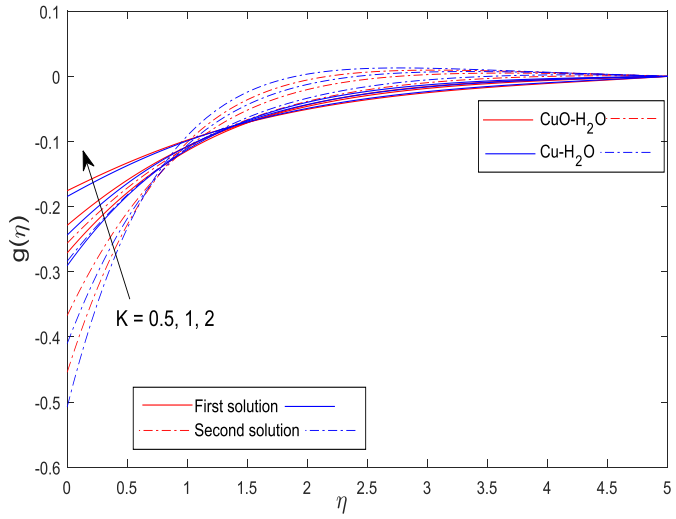

Figure 6. Angular velocity distribution $g(\eta)$ for developing values of K.

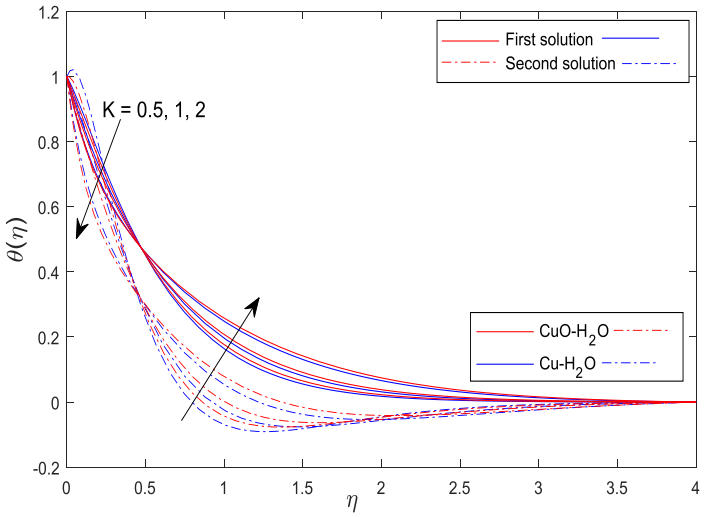

Figure 7. Temperature distribution $\theta(\eta)$ for developing values of K.

The influence of volume fraction (ϕ) of the nanoparticles on the fluid properties is discussed in Figs. (8)-(10). Due to the effects of ϕ, the magnitude of the angular velocity and temperature distributions are accelerated in both the cases [see Fig. (9) and Fig. (10)]. But, the magnitude of the velocity distribution of the fluid has been reduced due to the influence of ϕ (see Fig. 8). Physical explanations show that the effective viscosity of the micropolar fluid can change when the volume fraction of nanoparticles is increased. It can be more difficult for the fluid to flow when the volume percentage of microparticles increases, since this can cause the effective viscosity to rise. A decrease in velocity may result from this enhancement of viscosity. From figure (10), it is observed that water-based Cu micropolar nanofluid is better for heat transfer than $CuO - H_2O$. That is gain in volume fraction progresses the thermal transference of both liquids. The nanoparticles physically disperse energy in the form of heat. The improving values of volume fraction of the nanoparticles can exert additional energy and hence the temperature of the nanofluids enriches. But, this flow parameter accelerates the magnitude of the angular velocity distribution of the nanofluid [see Fig. 9]. Maximum variation of the angular velocity distribution in both the solutions has happened in the vicinity of the surface of the sheet. Also, it is noticed that the magnitude of the angular velocity of the fluid containing Cu is higher than the fluid holding Cu particle. The volume fraction of the nanoparticles

increases along with their contribution to the fluid's overall angular momentum. The angular velocity of the fluid may rise as a result.

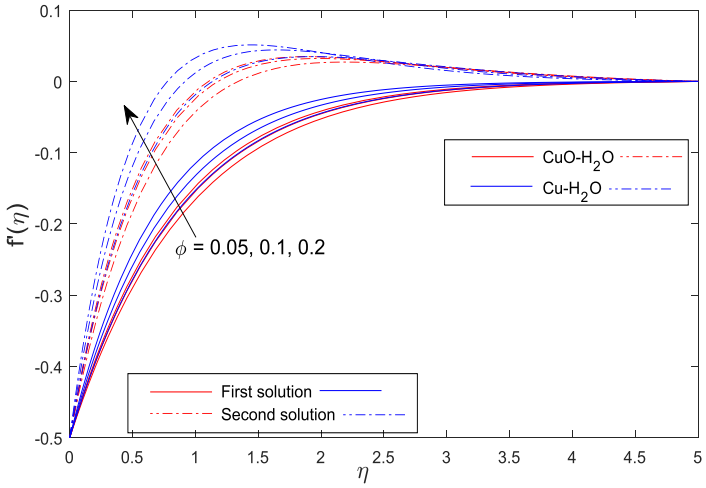

Figure 8. Velocity distribution $f'(\eta)$ for developing values of ϕ.

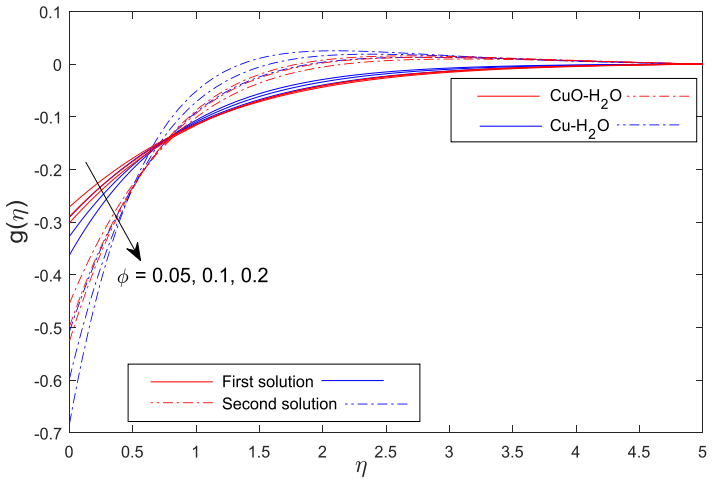

Figure 9. Angular velocity distribution $g(\eta)$ for developing values of ϕ.

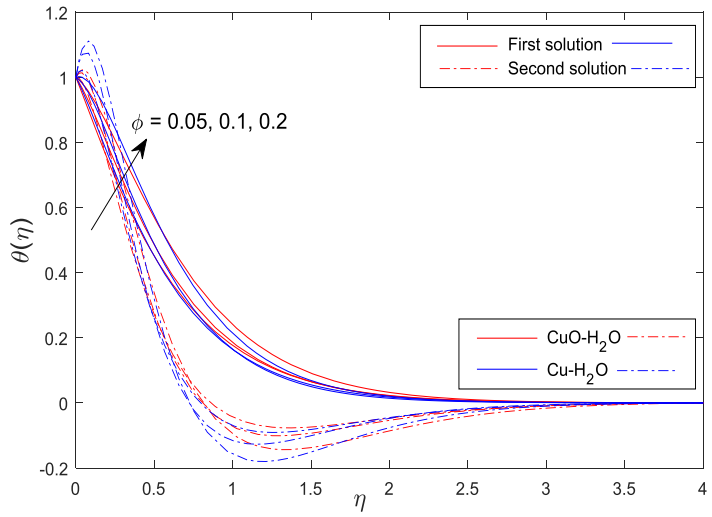

Figure 10. Temperature distribution $\theta(\eta)$ for developing values of ϕ.

From the above figures, it is discerned that all the figures exhibit dual solutions up to some certain region of the similarity variable η. Also, these figures satisfy the far-field boundary conditions asymptotically. The following Table-3 is established to show the stable and unstable solutions between the dual solutions with the help of evaluated least eigenvalues. From this table, it is perceived that the least eigenvalues for the first solutions of the nanofluid containing the metallic nanoparticles Cu and CuO are positive whereas, the least eigenvalues for the second solutions are negative. Due to the positive least eigenvalues, the initial disturbances in the fluid flow lie down that is $e^{-\omega\tau} \to 0, \omega > 0$ as time evolves $(\tau \to \infty)$. Hence, the first solutions are found stable. But, the least negative eigenvalue indicates the growth of initial disturbances in the flow that is $e^{-\omega\tau} \to \infty$and hence the flow solutions (second solution) are being as unstable behaviour.It is also perceived that all the flow profiles satisfy the far-field boundary conditions asymptotically and exist dual solutions up to the certain region of the similarity variables.

Tables- (4)-(6) are presented to examine the physical quantities that are observed in this study with different flow parameters. In the present problem, we have achieved three dimensionless quantities viz., skin friction coefficient $(f''(0))$, couple stress $(g'(0))$ and Nusselt number $(-\theta'(0))$. From table (4), we have concluded that the numerical values of the skin friction coefficient for first and second solutions are enhanced for different values of ϕduring the cases $(Cu - H_2O \& CuO - H_2O)$ when nanoparticles are suspended in water with the micropolar fluid model. But, the material parameter (K) which is responsible for the present fluid model reduces the skin friction coefficient during both cases. The volume fraction parameter (ϕ) rises the first and second solutions of couple stress values of the nanofluid [see Table-5]. It is also observed that the material parameter helps to control the values of couple stress at the surface of the sheet. The heat transfer rate $(-\theta'(0))$ of the nanofluid at the surface of the sheet is controlled with ϕ during both the cases (first and second solutions). But, the present fluid model is very useful to enhance the heat transfer rate [see Table-6]. From tables (4) and (5), it is also perceived that the numerical values of skin friction coefficients and couple stress of $Cu - H_2O$ are higher in comparison to the fluid containing CuO. But, an opposite nature is scrutinized in table (6) during the first and second solutions.

Table-3. Numerical values of least eigenvalue (ω) for various values of ϕ when $s = 1.23, M = 0.5, \mathrm{Pr} = 7, K = 0.5, n = 0.5, \lambda = -0.5, Ec = 3.$

ϕ	Least eigen-values (ω)			
	$Cu - H_2O$		$CuO - H_2O$	
	First solution	Second solution	First solution	Second solution
0.05	0.0174	-0.0581	0.0036	-0.2156
0.1	0.0123	-0.1086	0.0156	-2.3064
0.2	0.1893	-0.2256	0.0576	-2.5610

Table-4. Numerical values of drag force $(f''(0))$ at the surface for different values of flow parameters when $Pr = 7, M = 0.5, s = 1.23, \lambda = -0.5, n = 0.5, Ec = 10$.

ϕ	K	Skin friction coefficient $(f''(0))$			
		$Cu - H_2O$		$CuO - H_2O$	
		First solution	Second solution	First solution	Second solution
0.05	0.5	0.5815866559	1.0156281129	0.5422398188	0.9088982032
0.1		0.6541169996	1.1948185368	0.5787842511	0.9967087250
0.2		0.7250053144	1.3659980012	0.6026387732	1.0521881674
0.05	1	0.4874942920	0.8206699245	0.4575128755	0.7346638240
	2	0.3689237901	0.5677767403	0.3512518839	0.5123770477
	3	0.2997400494	0.4178849732	0.2893166144	0.3834993950

Table-5. Numerical values of couple stress $(g'(0))$ at the surface for different values of flow parameters when $Pr = 7, M = 0.5, s = 1.23, \lambda = -0.5, n = 0.5, Ec = 10$.

ϕ	K	Couple stress $(g'(0))$			
		$Cu - H_2O$		$CuO - H_2O$	
		First solution	Second solution	First solution	Second solution
0.05	0.5	0.2561009198	0.7286601526	0.2150338249	0.5808715033
0.1		0.3365534815	1.0124307145	0.2487457279	0.6998882426
0.2		0.4244192755	1.3274654106	0.2685512095	0.7789196405
0.05	1	0.1815418652	0.4804201826	0.1556632535	0.3852626822
	2	0.1023081265	0.2348104628	0.0909044929	0.1913441200
	3	0.0650960075	0.1272112146	0.0597708915	0.1063752578

Table-6. Numerical values of heat transfer rate $(-\theta'(0))$ at the surface for different values of flow parameters when $Pr = 7, M = 0.5, s = 1.23, \lambda = -0.5, n = 0.5, Ec = 10$.

ϕ	K	Heat transfer rate $(-\theta'(0))$			
		$Cu - H_2O$		$CuO - H_2O$	
		First solution	Second solution	First solution	Second solution
0.05	0.5	0.9507649048	-1.3064912036	1.2711682016	-0.0939126544
0.1		0.2651643344	-2.8449156712	0.7727309860	-0.9685290565
0.2		-0.1967546660	-3.1282005432	0.3617341766	-1.0920933372
0.05	1	1.6779747035	1.0868600760	1.9173941353	2.0414406632
	2	2.5316929610	4.1104226403	2.6591172981	4.6669267215
	3	2.9171874332	5.6745188988	2.9784201121	5.9518095236

4. Conclusion:

The following points are the major conclusions of this study.

1. The velocity and temperature distributions of $Cu - H_2O$ during both the solutions for different values of flow parameters are larger than $CuO - H_2O$.
2. But, the angular velocity distributions of fluid containing CuO are comparatively larger than Cu.
3. Due to the effects of the volume fraction parameter, the motion, as well as the temperature of the nanofluid enhance, but it decelerates the angular velocity of the fluid.
4. One of the most important advantages of this fluid model is that the material parameter reduces the shear stress at the surface of the sheet and enhances the heat transfer rate.

5. The shear stress of the nanofluid containing Cu-nanoparticle at the surface during both the solutions are comparatively smaller than the nanofluid suspending the CuO-nanoparticle with the effects of flow parameters such as volume fraction and material parameter.
6. From the stability point of view, the first solution is stable and the second solution is unstable and not physically tractable.
7. Researchers may extend this work by using different nanoparticles and different fluid models.

"Nomenclature

N	angular velocity(rad/s)
C_n	couple stress
A, B, C, D	constants
n	constant
f	dimensionless stream function
g	dimensionless angular velocity
Ec	Eckert number
B_0	magnetic field$(Tesla)$
M	magnetic parameter
K	material parameter
j	microinertia density(m^2)
Nu	Nusselt number
Pr	Prandtl number
C_p	specific heat at constant pressure(J/kgK)
s	suction/injection parameter
C_f	skin friction coefficient
T	temperature of the fluid (K)
t	time(s)
u	velocity along x-axis(m/s)
v	velocity along y-axis(m/s)
k	vortex viscosity(kg/ms)

Greek Symbols

ρ	density(kg/m^3)
μ	dynamic viscosity(kg/ms^2)
θ	dimensionless temperature
σ	electrical conductivity(s/m)
ν	kinematic viscosity(m^2/s)
λ	stretching/shrinking parameter
ψ	stream function
γ	spin gradient viscosity(kgm/s)
η	similarity variable
α	thermal diffusivity(m^2/s)
τ	time variable
ω	unknown eigenvalue
ϕ	volume fraction of the nanoparticles

Subscripts

f	base fluid
s	solid particle
nf	nanofluid

w	condition at the surface
∞	ambient condition"

Conflicts of Interest: The authors declare no conflicts of interest.

References:

[1] Choi, S. U. S.: Enhancing thermal conductivity of uids with nanoparticles. in *Pro- ceedings of the 1995 ASME Int. Mech. Eng. Cong. and Exposition, San Francisco, USA, ASME FED 231/MD*, pp. 99–105 (1995).

[2] Grigore, M. E.,Biscu, E. R., Holban, A. M., Gestal, M. C. and Grumezescu, A. M.: Methods of synthesis, properties and biomedical applications of CuO nanoparticles.*Pharmaceuticals, 9(4)*, pp. 1–14 (2016).

[3] Chanie, A. G., Shankar, B. and Nandeppanavar, M. M.: MHD flow of nanofluids through a porous media due to a permeable stretching sheet.*J. Nanofluids, 7(3)*, pp. 488–498 (2018).

[4] Ismail, H. N., Megahed, A. A., Abdel-Wahed, M. S. and Omama, M.: Thermal radiative effects on MHD casson nanofluid boundary layer over a moving surface. *J. Nanofluids*, 7(5), pp. 910–916 (2018).

[5] Gaikwad, S. N. and Chillal, S.: Radiation effect on MHD mixed convective flow of CU/CUO-water nanofluids in the presence of chemical reaction.*J. Nanofluids*, 7(3), pp. 509–515 (2018).

[6] Prasad, P. D., R. V. M. S. S., Kumar, K. and Varma, S. V. K.: Heat and mass transfer analysis for the MHD flow of nanofluid with radiation absorption.*Ain Shams Eng. J.*, 9(4), pp. 801–813 (2018).

[7] Muhammad, S., Khan, H., Ali, G., Ali Shah, S. I., Ishaq, M. and Hussain, S. A.: Stagnation point nanofluid flow of Cu and Ag nanoparticles over a stretching surface with magnetic effects. *J. Nanofluids*, 8(6), pp. 1314–1318 (2019).

[8] Molli, S. and Naikoti, K.: MHD Natural Convective Flow of Cu-Water Nanofluid over a Past Infinite Vertical Plate with the Presence of Time Dependent Boundary Condition.*Int. J. Thermofluid Sci. Technol.*, 7(4), pp. 1–15 (2020).

[9] Rajesh, V., Srilatha, M. and Chamkha, A. J.: Hydromagnetic effects on hybrid nanofluid (Cu–al2O3/Water) flow with convective heat transfer due to a stretching sheet.*J. Nanofluids*, 9(4), pp. 293–301 (2020).

[10] Tripathi, J., Vasu, B., Gorla, R. S. R., Chamkha, A. J., Murthy, P. V. S. N. and Bég, O. A.: Blood flow mediated hybrid nanoparticles in human arterial system: Recent research, development and applications. *J. Nanofluids*, 10(1), pp. 1–30 (2021).

[11] Sadeghi, M. S., Dogonchi, A. S., Ghodrat, M., Chamkha, A. J., Alhumade, H. and Karimi, N.: Natural convection of CuO-water nanofluid in a conventional oil/water separator cavity: Application to combined-cycle power plants. *J. Taiwan Inst. Chem. Eng.*, 124, pp. 307–319 (2021).

[12] Dogonchi, A. S., Sadeghi, M. S., Ghodrat, M., Chamkha, A. J., Elmasry, Y. and Alsulami, R.: Natural convection and entropy generation of a nanoliquid in a crown wavy cavity: Effect of thermo-physical parameters and cavity shape. *Case Stud. Therm. Eng.*, 27, p. 101208 (2021).

[13] Tayebi, T., Dogonchi, A. S., Karimi, N., Ge-JiLe, H., Chamkha, A. J. and Elmasry, Y.:Thermo-economic and entropy generation analyses of magnetic natural convective flow in a nanofluid-filled annular enclosure fitted with fins. *Sustain. Energy Technol. Assessments*, 46, p. 101274 (2021).

[14] Seyyedi, S. M., Dogonchi, A. S., Tilehnoee, M. H., Ganji, D. D. and Chamkha, A. J.: Second law analysis of magneto-natural convection in a nanofluid filled wavy-hexagonal porous enclosure. *Int. J. Numer. Methods Heat Fluid Flow*, 30(11), pp. 4811–4836 (2020).

[15] Krishna, M. V. and Chamkha, A. J.: Hall Effects on MHD Squeezing Flow of a Water-based Nanofluid Between Two Parallel Disks. *J. Porous Media*, 22(2), pp. 209–223 (2019).

[16] Eringen, A.: Theory of Micropolar Fluids. *Indiana Univ. Math. J.* (1966).

[17] Ariman, T., Turk, M. A. and Sylvester, N. D.: Applications of microcontinuum fluid mechanics. *Int. J. Eng. Sci.*,12(4), pp. 273–293 (1974).

[18] Anuradha, S. and Punithavalli, R.: MHD Boundary Layer Flow of a Steady Micro polar Fluid along a Stretching Sheet with Binary Chemical Reaction. *Int. J. App. Eng. Res.*, 14(2), pp. 440–446 (2019).

[19] Krishna, M. V., Anand, P. V. S. and Chamkha, A. J.: Heat and Mass Transfer on Free Convective Flow of Amicropolar Fluid Through A Porous Surface with Inclined Magnetic Field and Hall Effects. *Spec. Top. Rev. Porous Media An Int. J.*, 10(3), pp. 203–223 (2019).

[20] Hussain, S. T., Nadeem, S. and Haq, R. U.: Model-based analysis of micropolar nanofluid flow over a stretching surface. *European Physical Journal Plus, 129(8) (2014)*.

[21] Liana, E., Fauzi, A., Ahmad, S. and Pop, I.: Flow over a permeable stretching sheet in micropolar nanofluids with suction. *AIP Conference Proceedings 1605*, 428 (2015).

[22] Maripala, K., Srinivas and Naikoti: Development Research Chemical Reaction Effects on Micropolar Nanofluid Flow over a MHD Radiative Stretching Surface with Thermal Conductivity. *Int. J. Dev. Res.*, 6(12), pp. 10575–10581 (2016).

[23] Alizadeh, M., Dogonchi, A. S. and Ganji, D. D.: Micropolar nanofluid flow and heat transfer between penetrable walls in the presence of thermal radiation and magnetic field.*Case Stud. Therm. Eng.*,12(5), pp. 319–332 (2018).

[24] Dawar, A., Shah, Z., Kumam, P., Alrabiah, H., Khan, W., Islam, S. and Shaheem, N.: Chemically reactive MHD micropolar nanofluid flow with velocity slips and variable heat source/sink. *Sci. Rep.*, 10(1), pp. 1–23 (2020).

[25] Saleem, A., Sabih, W., Nadeem, S., Ghalambaz, M. and Issakhov, A.: Theoretical aspects of micropolar nanofluid flow past a deformable rotating cone.*Math. Methods Appl. Sci.*, June, pp. 1–19 (2020).

[26] Tayebi, T. and Chamkha, A. J.: Magnetohydrodynamic Natural Convection Heat Transfer of Hybrid Nanofluid in a Square Enclosure in the Presence of a Wavy Circular Conductive Cylinder. *J. Therm. Sci. Eng. Appl.*, 12(3), paper no. 031009 (2020).

[27] Chamkha, A.J., Dogonchi, A. S. and Ganji, D. D.: Magnetohydrodynamic Nanofluid Natural Convection in a Cavity under Thermal Radiation and Shape Factor of Nanoparticles Impacts: A Numerical Study Using CVFEM. *Appl. Sci.*, 8(12), p. 2396 (2018).

[28] Krishna, M. V. and Chamkha, A. J.: Hall and ion slip effects on MHD rotating boundary layer flow of nanofluid past an infinite vertical plate embedded in a porous medium. *Results Phys.*, 15, p. 102652 (2019).

[29] Krishna, M. V. and Chamkha, A. J.: MHD Peristaltic Rotating Flow of A Couple Stress Fluid Through A Porous Medium with Wall and Slip Effects. *Spec. Top. Rev. Porous Media An Int. J.*, 10(3), pp. 245–258 (2019).

[30] Crane, L. J.: Flow past a stretching plate.*Zeitschrift für Angew. Math. und Phys. ZAMP*, 21(4), pp. 645–647 (1970).

[31] Khan, W. A., Makinde, O. D. and Khan, Z. H.: Non-aligned MHD stagnation point flow of variable viscosity nanofluids past a stretching sheet with radiative heat. *Int. J. Heat Mass*

Transf., 96, pp. 525–534 (2016).

[32] Ghosh, S. andMukhopadhyay, S.: Flow and heat transfer of nanofluid over an exponentially shrinking porous sheet with heat and mass fluxes.*Propuls. Power Res.*, 7(3), pp. 268–275 (2018).

[33] Dey, D. and Borah, R.: Dual Solutions of Boundary Layer Flow with Heat and Mass Transfers over an Exponentially Shrinking Cylinder: Stability Analysis. *Lat. Am. Appl. Res.*, 50(4), pp. 247–253 (2020).

[34] Dey, D., Hazarika, M. and Borah, R.: Entropy Generation Analysis of Magnetized Micropolar Fluid Streaming above an Exponentially Extending Plane. *Lat. Am. Appl. Res.*, 51(4) (2021).

[35] Dey, D. and Chutia, B. Dusty nanofluid flow with bioconvection past a vertical stretching surface. *J. King Saud Univ. - Eng. Sci*, (2020).

[36] Zehra, I., Abbas, N., Amjad, M., Nadeem, S., Saleem, S. and Issakhov, A.: Casson nanoliquid flow with Cattaneo-Christov flux analysis over a curved stretching/shrinking channel. *Case Stud. Therm. Eng.*, 27, p. 101146 (2021).

[37] Prasannakumara, B. C.: Numerical simulation of heat transport in Maxwell nanofluid flow over a stretching sheet considering magnetic dipole effect.*Partial Differ. Equations Appl. Math.*, 4(6), p. 100064 (2021).

[38] Jamshed, W., Devi, S.U., Goodrazi, M., Prakash, M., Nisar, K.S., Zakarya, M. and Abdel-Aty, A.H.: Evaluating the unsteady Casson nanofluid over a stretching sheet with solar thermal radiation: An optimal case study.*Case Stud. Therm. Eng.*, 26, p. 101160 (2021).

[39] Merkin, J. H.: On dual solutions occurring in mixed convection in a porous medium. *J. Eng. Math.*, vol. 20, no. 2, pp. 171–179 (1986).

[40] Anuar, N. S. and Bachok, N.: Double solutions and stability analysis of micropolar hybrid nanofluid with thermal radiation impact on unsteady stagnation point flow.*Mathematics*, 9(3), pp. 1–18 (2021).

[41] Dey, D. and Borah, R.: Stability analysis on dual solutions of second- grade fluid flow with heat and mass transfers over a stretching sheet. *Int. J. Thermofluid Sci. Technol.*, 8(2) (2021).

[42] Dey, D., Borah, R. and Mahanta, B.: Boundary Layer Flow and Its Dual Solutions Over a Stretching Cylinder: Stability Analysis. in *Emerging Technologies in Data Mining and Information Security. Advances in Intelligent Systems and Computing*, pp. 27–38 (2021).

[43] Waini, I., Ishak, A. and Pop, I.: Hiemenz flow over a shrinking sheet in a hybrid nanofluid. *Results Phys.*, 19 (8), p. 103351 (2020).

[44] Khashi'ie, N. S., Arifin, N. M., Pop, I. and Wahid, N. S.: Flow and heat transfer of hybrid nanofluid over a permeable shrinking cylinder with Joule heating: A comparative analysis. *Alexandria Eng. J.*, 59(3), pp. 1787–1798 (2020).

[45] Ahmadi, G. and Shahinpoor, M.: Universal stability of magneto-micropolar fluid motions.*Int. J. Eng. Sci.*, 12(7), pp. 657–663 (1974).

[46] Ahmed, S. E., Mansour, M. A., Mahdy, A. and Mohamed, S. S.: Entropy generation due to double diffusive convective flow of Casson fluids over nonlinearity stretching sheets with slip conditions. *Eng. Sci. Technol. an Int. J.*, 20(6), pp. 1553–1562 (2017).

[47] Mishra, G. S., Hussain, M.R., Makinde, O.D. and Seth, S.M.: Stability analysis and dual multiple solutions of a hydromagnetic dissipative flow over a stretching / shrinking sheet. *Bulg. Chem. Commun.*, 52(2), pp. 259–271 (2020).

[48] Togun, H., Homod, R.Z. and Abdulrazzaq, T.: HYBRID AL_2O_3-CU-WATER NANOFLUID-FLOW AND HEAT TRANSFER OVER VERTICAL DOUBLE FORWARD-FACING STEP. *Thermal Science*, 25(5A), pp. 3517-3529 (2021).

[49] Dey, D., Makinde, O.D. and Borah, R.: Analysis of Dual Solutions in MHD Fluid Flow with Heat and Mass Transfer Past an Exponentially Shrinking/Stretching Surface in a Porous Medium. *International Journal of Applied and Computational Mathematics., 8(66), (2022).*

Submitted: 28.01.2023.

Revised: 20.09.2023.

Accepted: 03.10.2023.